JOC The Journal of Organic Chemistry

Article

pubs.acs.org/joc

Dicarboxylate Recognition by Two Macrobicyclic Receptors: Selectivity for Fumarate over Maleate

Pedro Mateus,[†] Rita Delgado,*[,†] Paula Brandão,[‡] and Vítor Félix[§]

[†]Instituto de Tecnologia Química e Biológica, Universidade Nova de Lisboa, Av da República - EAN, 2780-157 Oeiras, Portugal

[‡]Departamento de Química, CICECO, Universidade de Aveiro, 3810-193 Aveiro, Portugal

[§]Departamento de Química, CICECO, and Secção Autónoma de Ciências da Saúde, Universidade de Aveiro, 3810-193 Aveiro, Portugal

Supporting Information

ABSTRACT: Two ditopic polyamine macrobicyclic compounds have been studied as receptors for the recognition of dicarboxylate anions of varying chain length in aqueous solution. One of the receptors consists of two tris(2-aminoethyl)amine-derived binding subunits separated by *p*-xylyl spacers, while the other is a heteroditopic compound, combining two different head units, a tren-derived and a 2,4,6-triethylbenzene-derived one, also separated by *p*-xylyl spacers. The acid−base behavior of the compounds as well as their binding ability with oxalate (oxa^{2-}), malonate (mal^{2-}), succinate (suc^{2-}), glutarate (glu^{2-}), maleate ($male^{2-}$) and fumarate (fum^{2-}) anions were studied by potentiometry at 298.2 K in aqueous solution and at ionic strength 0.10 M in KTsO. NMR studies were also performed to obtain structural information in solution on the supermolecules formed by association of the protonated macrobicycles with the dicarboxylate substrates. The results revealed that both compounds are able to form stable associations with the dianionic substrates in competitive aqueous solution, with unprecedented selectivity for fum^{2-} over other dicarboxylate competitors, including its *cis* isomer $male^{2-}$. In addition it was found that although the selectivity pattern is unaffected by the introduction of the 2,4,6-triethylbenzene head unit, the affinity toward dicarboxylates is significantly reduced. Therefore, the comparison between the binding behavior of these two receptors showed the effect of the increased rigidity and lipophilicity of the receptor with the 2,4,6-triethylbenzene head unit in the binding properties and the selectivity pattern.

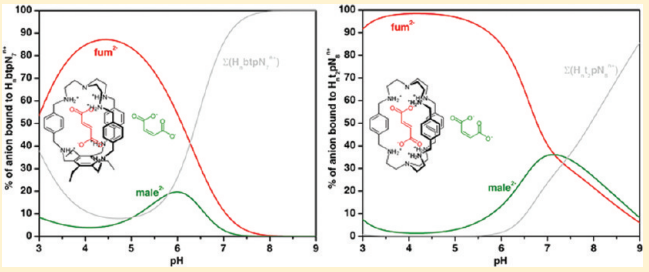

INTRODUCTION

The design of new synthetic receptors for carboxylate anions has interested supramolecular chemists since the early days of this relatively young field of research.[1] Indeed, the carboxylate functionality is part of a wide range of biologically and environmentally active entities, in many cases accounting for their chemical and biological properties.[2]

Dicarboxylates, in particular, are key intermediates of the Krebs cycle, the metabolic pathway used by all aerobic organisms for energy production. Fum^{2-} is one of such metabolic intermediates, formed by the oxidation of suc^{2-} by the enzyme succinate dehydrogenase, after which is converted by the enzyme fumarase to malate.[2] Mutations impairing the function of fumarase in humans cause accumulation of fum^{2-} and are related with the development of cutaneous and uterine leiomyomas and papilary renal cell cancer.[3] In addition, it was suggested that accumulation of fum^{2-} competitively inhibits the 2-oxoglutarate-dependent dioxygenases, activating oncogenic hypoxia pathways that lead to tumor formation predisposition.[4]

The design of a synthetic receptor that selectively binds fum^{2-} in the presence of structurally similar or isomeric competitors may have important applications. Indeed, it has been pointed out that sequestering a biological effector with a synthetic compound could represent an alternative or complementary strategy to the standard approach of creating small molecules that bind to biological macromolecules.[5]

In order to be suitable for such applications, synthetic receptors need to be able to strongly and selectively bind the substrate of interest in the most challenging medium in anion recognition: water.[6] Among the most successful groups of receptors for the binding of carboxylate anions in aqueous medium there are the polyamine compounds, as they can be protonated to provide the necessary positive charges to interact with the substrates and to impart water solubility.[7] Thus amino groups have been incorporated in a variety of different topologies, from linear structures to mono- and polycyclic architectures, and studied as receptors of carboxylates and other anions.[8] The ability of tris(2-aminoethyl)amine (tren) derived polyammonium cryptands to strongly bind anions in aqueous medium by combining electrostatic and hydrogen bonding interactions has been explored since the beginning of anion recognition as a research field.[8e,9] More recently, 2,4,6-triethylbenzene-derived

Received: February 20, 2012
Published: April 23, 2012

Chart 1. Macrobicyclic Compounds and Target Dicarboxylate Substrates Studied in This Work

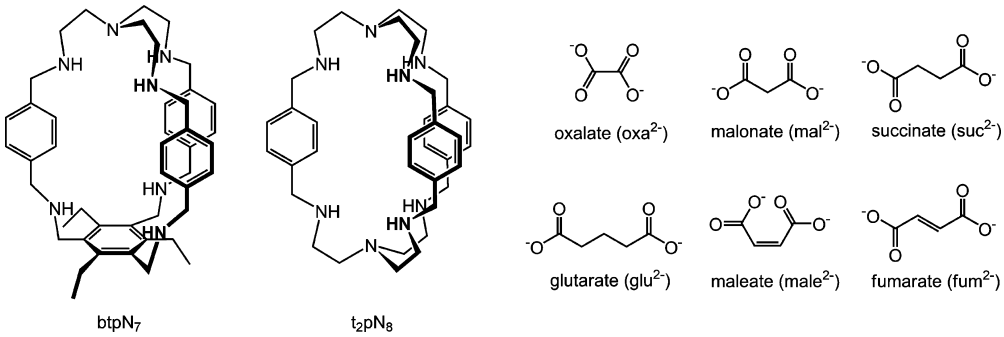

Table 1. Overall (β_i^H) and Stepwise (K_i^H) Protonation Constants of $btpN_7$ and t_2pN_8 in Aqueous Solution[a]

	log β_i^H[b]			log K_i^H	
equilibrium reaction	$btpN_7$	t_2pN_8	equilibrium reaction	$btpN_7$	t_2pN_8
$L + H^+ \rightleftharpoons HL^+$	8.99(1)	9.20(1)	$L + H^+ \rightleftharpoons HL^+$	8.99	9.20
$L + 2\,H^+ \rightleftharpoons H_2L^{2+}$	17.58(1)	18.16(1)	$HL^+ + H^+ \rightleftharpoons H_2L^{2+}$	8.59	8.96
$L + 3\,H^+ \rightleftharpoons H_3L^{3+}$	25.15(1)	25.93(1)	$H_2L^{2+} + H^+ \rightleftharpoons H_3L^{3+}$	7.57	7.77
$L + 4\,H^+ \rightleftharpoons H_4L^{4+}$	31.70(1)	33.13(1)	$H_3L^{3+} + H^+ \rightleftharpoons H_4L^{4+}$	6.55	7.20
$L + 5\,H^+ \rightleftharpoons H_5L^{5+}$	37.60(1)	38.37(1)	$H_4L^{4+} + H^+ \rightleftharpoons H_5L^{5+}$	5.90	5.24
$L + 6\,H^+ \rightleftharpoons H_6L^{6+}$	42.88(1)	43.49(1)	$H_5L^{5+} + H^+ \rightleftharpoons H_6L^{6+}$	5.28	5.12

[a] T = (298.2 ± 0.1) K and I = (0.10 ± 0.01) M in KTsO. [b] Values in parentheses are standard deviations in the last significant figures.

polyammonium macrobicycles have also shown interesting anion-binding properties.[10]

In this work, the binding properties of the protonated forms of two closely related polyamine cryptands, $btpN_7$ and t_2pN_8, toward dicarboxylate substrates have been studied in aqueous solution (Chart 1). We expected that these compounds would be selective for fum^{2-} in the presence of other dicarboxylates, including its *cis* isomer $male^{2-}$, given their ditopic nature and the length of the *p*-xylyl spacer. The selective recognition of an isomer over the other is, in general, a challenging task due to their similar chemical and physical properties. Indeed only few receptors were reported that discriminate *cis*/*trans* isomers $male^{2-}$ and fum^{2-}, all of them showing selectivity for $male^{2-}$ over fum^{2-} and working only in non aqueous solvents.[11] In fact, to the best of our knowledge, there are no synthetic receptors selective for fum^{2-} in aqueous solution.

In addition, studying these closely related receptors gives the opportunity to monitor the change on the thermodynamics of binding as a response to a structural change such as the replacement of a tren by a 2,4,6-triethylbenzene head unit of the receptor, corresponding to an increased rigidity and lipophilicity.

RESULTS AND DISCUSSION

Acid–base Behavior of $btpN_7$ and t_2pN_8. The protonation constants of the compounds $btpN_7$ and t_2pN_8 were determined by potentiometry in aqueous solution at 298.2 K and ionic strength 0.10 M in KTsO. The results are collected in Table 1 and the corresponding species distribution diagrams represented in Figure 1.

The bulky potassium tosylate (KTsO) salt was chosen as supporting electrolyte based on the assumption that it does not appreciably interact with the receptors.[10b,c,12] Indeed, it was found that using KBr or KNO_3[13] (Table S1 in the Supporting Information) as supporting electrolyte increased the protonation constants of $btpN_7$ relative to those determined in KTsO, specially the lower constants, indicative of stronger association with Br^- and NO_3^- than with TsO^-. In addition, the crystal structure of $[H_6t_2pN_8(H_2O)_3](TsO)_6{\cdot}4H_2O$ showed the tosylate counterions outside of the receptor cavity.[14]

Six protonation constants were found for both compounds in the working pH region (3.0–10.0), corresponding to the successive protonations of the secondary amines. The stepwise values decrease with increasing protonation state of the receptors due to both increasing electrostatic repulsion between positive charges and to statistical factors. The protonation constant of the tertiary amine of the tren derived head unit of $btpN_7$, as well as the protonation of both tertiary amines of t_2pN_8, are not obtained in the studied pH region, which should be very acidic due to the accumulation of positive charges within the receptors cavities. The constants have similar magnitude in pairs, as they correspond to protonation of amine centers at alternating positions in the macrobicyclic backbone, far from each other, and therefore the differences in values for each pair are mainly due to statistical factors. This behavior is clearer in t_2pN_8 than in $btpN_7$ because the secondary amines in the 1,3,5-tris(aminomethyl)-2,4,6-triethylbenzene subunit have lower basicity than those of the tris(2-aminoethyl)amine part, due to the electron-withdrawing effect of the nearby benzene ring. Nonetheless, the overall basicity of these two compounds is quite similar, and as shown in Figure 1, the H_6 $btpN_7^{6+}$ and $H_6t_2pN_8^{6+}$ species exist as the main species at pH values lower than 5.0.

X-ray Crystal Structures. The crystal structure of the oxa^{2-} association with $H_6btpN_7^{6+}$ is built up from an asymmetric unit composed of three oxa^{2-} anions, one $H_6btpN_7^{6+}$, and thirteen water molecules, two of these water molecules are inserted into the cryptand cavity, which is consistent with the molecular formula $[H_6btpN_7(H_2O)_2](oxa)_3{\cdot}11H_2O$. As can be seen in Figure 2 (right view), in the crystal structure each $H_6btpN_7^{6+}$ is surrounded by six oxa^{2-} anions, from which five interact directly with nine of twelve N–H receptor binding sites available for N–H···O hydrogen bonds. The N···O distances of these interactions range from 2.790(2) to 3.059(2) Å. Furthermore,

dx.doi.org/10.1021/jo300320w | J. Org. Chem. 2012, 77, 4611–4621

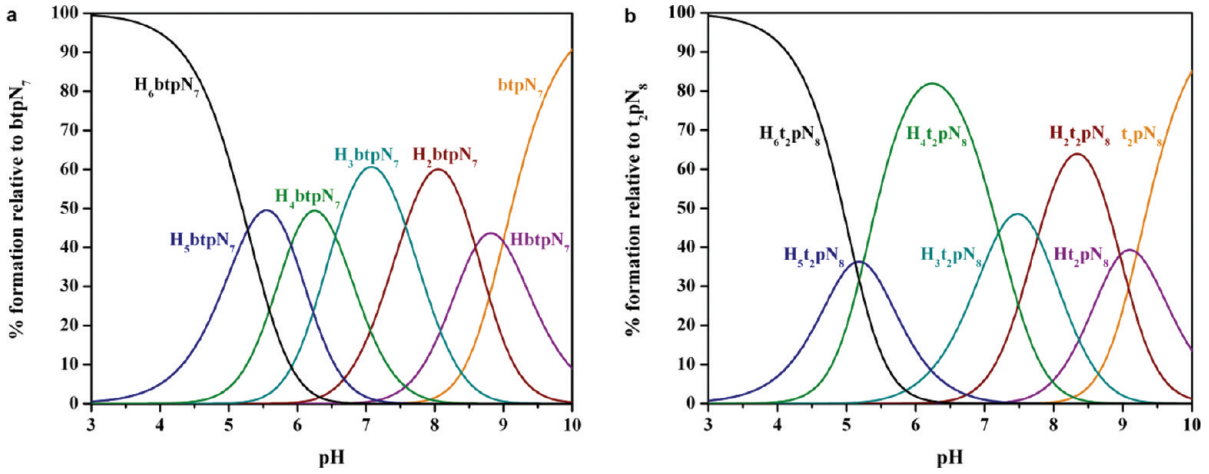

Figure 1. Species distribution diagrams of the protonation of $btpN_7$ (a) and t_2pN_8 (b). $C_{btpN_7} = C_{t_2pN_8} = 1.0 \times 10^{-3}$ M. Charges were omitted.

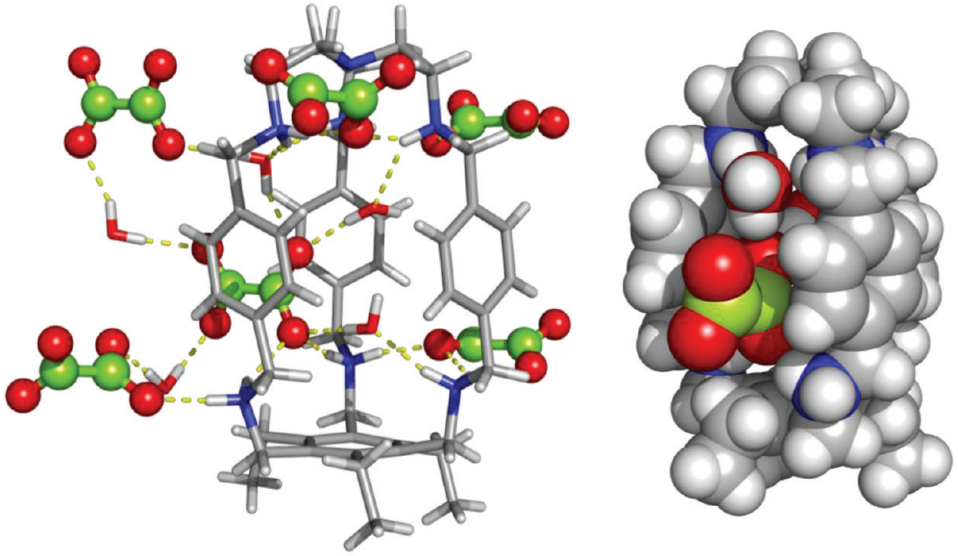

Figure 2. Perspective views of $[H_6btpN_7(H_2O)_2](oxa)_3 \cdot 11H_2O$ association showing different structural features: (a) $[H_6btpN_7(H_2O)_2]^{6+}$ surrounded by six oxa^{2-} anions; (b) space-filling model showing one oxa^{2-} almost inserted into the cryptand cavity together with two water molecules.

one of these anions is almost hosted inside of the cryptand cavity (see Figure 2b) with two oxygen atoms from one carboxylate group forming three concomitant O−H···O hydrogen bonds, two with encapsulated water molecules [O···O distances of 2.745(2) and 2.722(3) Å], and one with the water molecule closest to the receptor cavity [O···O distance of 2.728(2) Å]. These three hydrogen bonds together with two N−H···O bonding interactions maintain the anion firmly bound to the $H_6btpN_7^{6+}$ receptor. This embed anion is also hydrogen bonded to the sixth oxa^{2-} via two water bridges as shown in Figure 2a. Among the remaining three N−H binding sites, two neighbors are involved in two independent hydrogen bonds with a water molecule, which is located near the receptor cavity at N···O distances of 2.782(2) and 2.812(2) Å. The last N−H binding site available is hydrogen bonded to an encapsulated water molecule with N···O distance of 2.959(2) Å. Indeed, in the solid state, all oxygen atoms of carboxylate anions, water crystallization molecules and N−H binding sites of the $H_6btpN_7^{6+}$ receptor are assembled into a complex 3-D network of hydrogen bonding interactions. The dimensions of these −C═O···H−O, O−H···OH_2, N−H···OH_2, and −C═O···H−N hydrogen bonds are listed in Table S2 in the Supporting Information. A further insight into the crystal packing presented in Figure S1 in the Supporting Information also shows that adjacent $H_6btpN_7^{6+}$ molecules are assembled with the 2,4,6-triethylbenzene caps or tren moieties of nearby receptor molecules adopting a "head-to-head" arrangement. In contrast with hydrophobic 2,4,6-triethylbenzene subunits, a network of hydrogen bonds composed of water molecules and oxa^{2-} anions separates the hydrophilic tren subunits.

The crystal structure of the fum^{2-} association with $H_nbtpN_7^{n+}$ receptor is assembled from an asymmetric unit containing one receptor molecule and 2.5 fum^{2-} anions. This means that the cryptand is pentaprotonated ($H_5btpN_7^{5+}$) in agreement with the charge balance of the compound. The nonprotonated secondary nitrogen atom was ascertained as described below in the Experimental Section. The asymmetric unit content is completed with 25 water molecules, six of them with half occupancy as

dx.doi.org/10.1021/jo300320w | J. Org. Chem. 2012, 77, 4611−4621

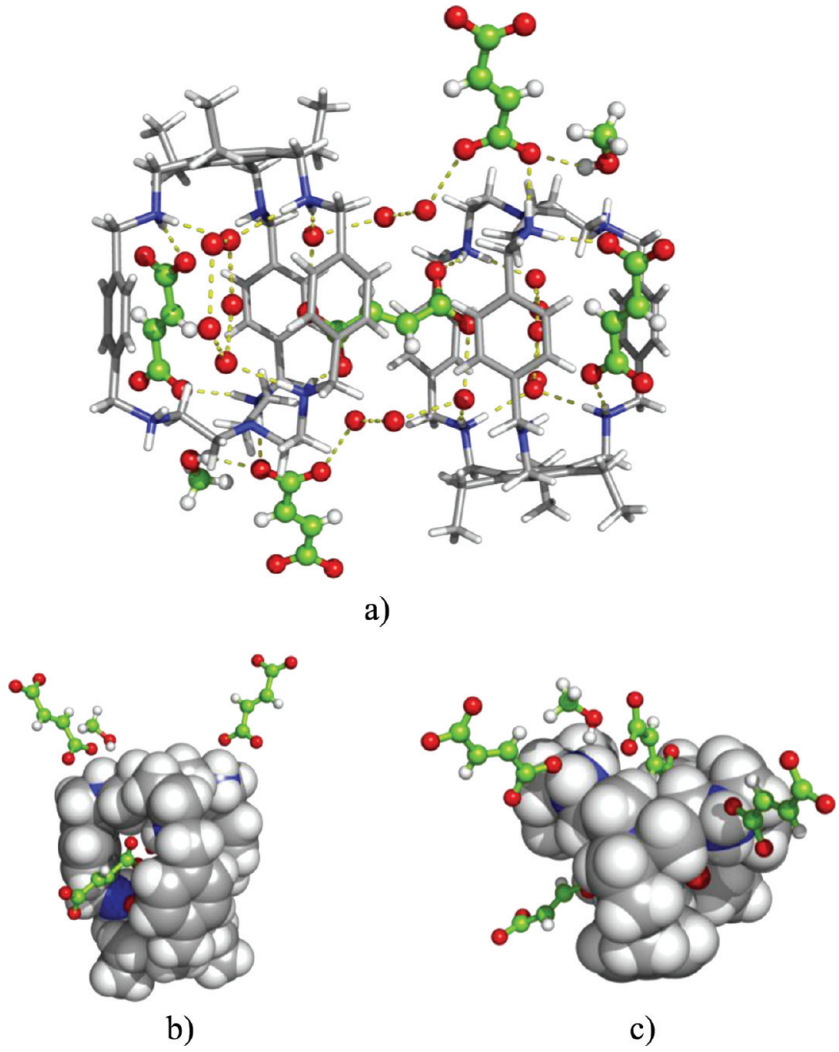

Figure 3. Relevant structural features found in the crystal packing of $[(H_5btpN_7(H_2O)_4)_2(fum)_5]\cdot 36H_2O\cdot MeOH$. (a) Centrosymmetric assembly of two $H_5btpN_7^{5+}$ and five fum^{2-} anions. (b) and (c) $H_5btpN_7^{5+}$ cation represented in a space-filling model emphasizing the encapsulation of four water molecules and one carboxylate group of two fum^{2-} anions. The O···H−N hydrogen bonds and O···O short contacts are drawn as yellow dashed lines.

well as one crystallization methanol molecule, which is consistent with the molecular formula $[(H_5btpN_7(H_2O)_4)_2(fum)_5]\cdot 36H_2O\cdot MeOH$. Indeed, the fum^{2-} with half occupancy is located on an inversion crystallographic center and bridges two $H_5btpN_7^{5+}$ molecules via O···H−N bonding interactions in the centrosymmetric assembly depicted in Figure 3a. In contrast with X-ray single-crystal structure of the oxa^{2-} association, the water hydrogen atoms were not discernible from difference Fourier maps limiting the detailed analysis of the hydrogen bonds to the O···H−N bonding interactions gathered in Table S3 in the Supporting Information. Furthermore, two water molecules were found disordered over two positions with equal probability. However, O···O close contact distances found indicate that in the solid state the crystallization water molecules, $H_5btpN_7^{5+}$ cation and the fum^{2-} anions are also assembled into a complex 3-D network of hydrogen bonds. One fum^{2-} anion is located at the entrance of the cavity, establishing two independent O···H−N hydrogen bonds, one with a N−H binding site adjacent to the 2,4,6-triethylbenzene cap with a O···N distance of 2.642(8) Å and the other with a N−H group from the tren subunit with a O···N distance of 2.715(4) Å. In contrast, the remaining two anions interact directly with the heteroditopic receptor by a single O···H−N hydrogen bond with O···N distances of 2.713(4) and 2.685(4) Å, respectively. Besides the fum^{2-} bridge showed in Figure 3a, the neighboring $H_5btpN_7^{5+}$ molecules are linked by a second fum^{2-} bridge in such way that each $H_5btpN_7^{5+}$ is O···N−H hydrogen bonded to four fum^{2-} anions, as can be seen in Figure 3c. The $H_5btpN_7^{5+}$ also hosts one water molecule in the middle of the cryptand cavity and is surrounded by three water molecules hydrogen bonded to NH_2 binding groups with O···N distances between 2.839(5) and 2.876(4) Å. Moreover, three fum^{2-} anions are also connected by water bridges or methanol molecules located on the receptor periphery.

Binding Affinity of $H_nbtpN_7^{n+}$ and $H_nt_2pN_8^{n+}$ Receptors toward Dicarboxylate Substrates. The association constants of the protonated forms of $btpN_7$ and t_2pN_8 with several dicarboxylate anions differing in chain length were determined by potentiometry, in aqueous solution, at 298.2 K and 0.10 M KTsO. The values are collected in Table 2. The protonation constants of the dicarboxylates were also determined in the same experimental conditions and used in the calculations (Table S4 in the Supporting Information).

Only species of 1:1 receptor to anion stoichiometry were found for the different protonation states of both compounds. The larger association constants were found to correspond to

dx.doi.org/10.1021/jo300320w | J. Org. Chem. 2012, 77, 4611−4621

Table 2. Stepwise Association Constants (log $K_{H_hL_tA_a}$) of $H_nbtpN_7^{n+}$ and $H_nt_2pN_8^{n+}$ Receptors with oxa^{2-}, mal^{2-}, suc^{2-}, glu^{2-}, $male^{2-}$, and fum^{2-} Anions in Aqueous Solution[a–c]

reaction equilibrium[d]	oxa^{2-}	mal^{2-}	suc^{2-}	glu^{2-}	$male^{2-}$	fum^{2-}
$H_6btpN_7^{6+} + HA^- \rightleftharpoons [H_7btpN_7A]^{5+}$	2.37(2)	2.25(2)			1.89(3)	2.60(4)
$H_6btpN_7^{6+} + A^{2-} \rightleftharpoons [H_6btpN_7A]^{4+}$	4.04(1)	3.66(1)	3.08(1)	2.57(1)		3.89(1)
$H_5btpN_7^{5+} + HA^- \rightleftharpoons [H_6btpN_7A]^{4+}$					2.97(2)	
$H_5btpN_7^{5+} + A^{2-} \rightleftharpoons [H_5btpN_7A]^{3+}$	2.89(1)	2.64(2)	2.04(3)	2.11(2)	2.79(1)	2.85(3)
$H_4btpN_7^{4+} + A^{2-} \rightleftharpoons [H_4btpN_7A]^{2+}$		2.18(3)	1.87(3)	1.92(3)		2.17(6)
$H_6t_2pN_8^{6+} + HA^- \rightleftharpoons [H_7t_2pN_8A]^{5+}$	4.77(2)	3.52(2)	3.35(1)	2.99(2)	3.50(2)	
$H_6t_2pN_8^{6+} + A^{2-} \rightleftharpoons [H_6t_2pN_8A]^{4+}$	6.21(1)	5.35(1)	4.63(1)	3.85(1)		6.06(1)
$H_5t_2pN_8^{5+} + HA^- \rightleftharpoons [H_6t_2pN_8A]^{4+}$					4.44(2)	
$H_5t_2pN_8^{5+} + A^{2-} \rightleftharpoons [H_5t_2pN_8A]^{3+}$	3.77(6)	3.83(2)	3.45(2)	3.25(2)		4.02(3)
$H_4t_2pN_8^{4+} + HA^- \rightleftharpoons [H_5t_2pN_8A]^{3+}$					3.40(2)	
$H_4t_2pN_8^{4+} + A^{2-} \rightleftharpoons [H_4t_2pN_8A]^{2+}$	2.45(3)	2.68(1)	2.68(1)	2.67(2)	2.81(1)	2.73(2)
$H_3t_2pN_8^{3+} + A^{2-} \rightleftharpoons [H_3t_2pN_8A]^{+}$	2.18(3)	2.39(2)	2.33(2)	2.28(3)	2.53(2)	2.44(3)
$H_2t_2pN_8^{2+} + A^{2-} \rightleftharpoons [H_2t_2pN_8A]$		1.60(5)	1.69(4)	1.65(7)	1.87(3)	1.72(6)

[a] T = (298.2 ± 0.1 K) and I = (0.10 ± 0.01) M in KTsO. [b] Values in parentheses are standard deviations in the last significant figures. [c] Values of the overall association constants are presented in Table S5 in the Supporting Information. [d] A^{2-} denotes in general the dicarboxylate anion.

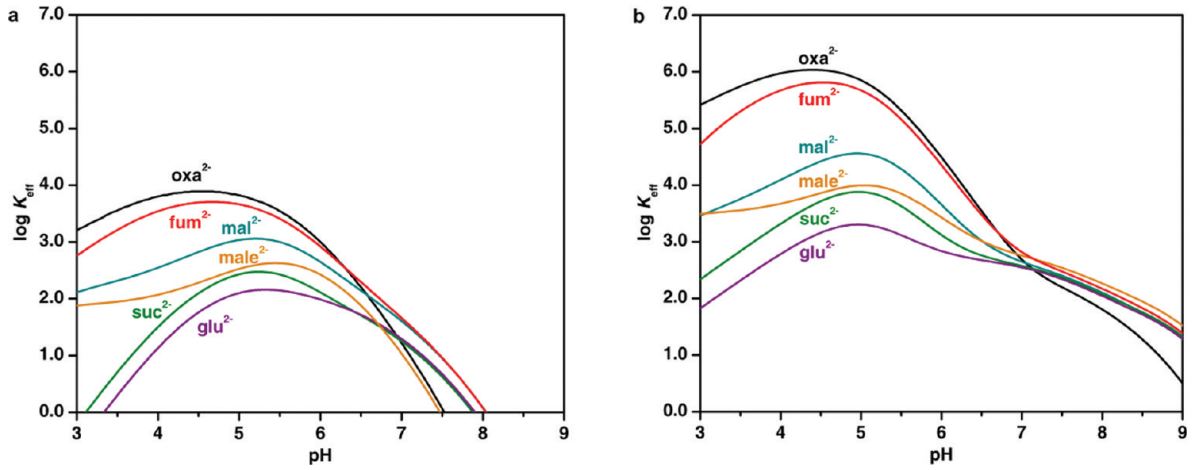

Figure 4. Plots of the log K_{eff} versus pH for the associations formed between the indicated dicarboxylate anions and the receptors $H_nbtpN_7^{n+}$ (a) or $H_nt_2pN_8^{n+}$ (b).

the association of the hexaprotonated receptors with the fully ionized dicarboxylates, with the exception of $male^{2-}$. The latter anion, being more basic (see Table S4 in the Supporting Information), does not exist in the fully deprotonated form in the pH region where both receptors are hexaprotonated. It was also found that the association constants decrease with decreasing protonation of the receptors and with increasing protonation of the substrates, clearly indicating that electrostatic interactions and hydrogen bonds play a significant role in the binding process.

The $H_nt_2pN_8^{n+}$ receptor binds to all substrates with larger association constants than $H_nbtpN_7^{n+}$. Because of differences in basicity of receptors, direct comparison of stepwise constants may be misleading. Likewise, the differences in basicity of the studied dicarboxylates can give rise to incorrect selectivity attributions, especially when there are overlapping protonation equilibria between receptors and anions. The K_{eff} value is defined as the quotient between the total concentration of supramolecular species formed and the product of the total concentration of the free receptor and the total concentration free substrate at a given pH ($K_{eff} = \Sigma[H_{i+j}LA]/\Sigma[H_iA]\ \Sigma[H_jL]$, where L is the deprotonated receptor and A the anion), provides a better way to visualize the affinity of the receptor for each anion along the pH region.[15] These values not only allow comparisons between different supramolecular systems studied under the same experimental conditions, as it takes into consideration the different basicities of receptors and substrates, but also provides helpful guides to distinguish the stepwise equilibria that effectively occur from all those that can be established for each case. In Figure 4 are shown the plots of the effective association constant K_{eff} versus pH for the supramolecular associations between the protonated forms of $btpN_7$ and t_2pN_8 and the studied dicarboxylates.

From these plots it is clear that $H_nt_2pN_8^{n+}$ binds all the dicarboxylate anions significantly stronger than $H_nbtpN_7^{n+}$, a result which was somewhat unexpected given the structural and basicity similarities of both compounds. However, at pH ≈ 4.5, where the interactions of the two receptors with the substrates reach the maximum strength, the sequence of binding preference is the same (oxa^{2-} > fum^{2-} > mal^{2-} > $male^{2-}$ > suc^{2-} > glu^{2-}). Indeed, the competitive binding diagrams[16] plotted for the association of each compound with the studied dicarboxylates (Figure 5) show that their selectivity pattern is practically identical. Thus, the much higher affinity of $H_nt_2pN_8^{n+}$ toward dicarboxylates relative to $H_nbtpN_7^{n+}$ does not translate into higher selectivity when all of the studied anions are considered.

dx.doi.org/10.1021/jo300320w | J. Org. Chem. 2012, 77, 4611–4621

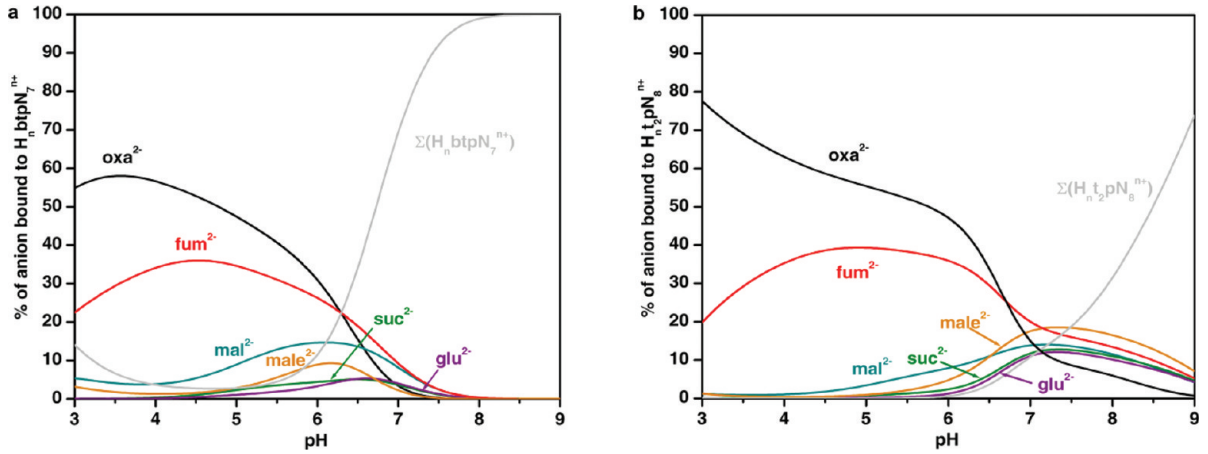

Figure 5. Distribution diagrams of the overall amounts of supramolecular species formed between the dicarboxylate anions and the receptors $H_nbtpN_7^{n+}$ (a) and $H_nt_2pN_8^{n+}$ (b), in equimolar ratio. $C_{btpN_7} = C_{t_2pN_8} = C_A/3 = 1.0 \times 10^{-3}$ M. For simplicity, the amount of associated species with each anion, $[H_nLA]^{(n-2)+}$, is identified in the diagrams only by the formula of the anions, oxa^{2-}, mal^{2-}, suc^{2-}, glu^{2-}, $male^{2-}$, and fum^{2-}, respectively.

The selectivity trend observed does not strictly follow the sequence of acidity of the substrates (oxa^{2-} > fum^{2-} > glu^{2-} > suc^{2-} > mal^{2-} > $male^{2-}$), which means that structural factors also play a role in the binding behavior.

In both cases, oxa^{2-} and fum^{2-} display higher association constants than the rest of the substrates. Due to the small size of the oxa^{2-} anion, it seems unlikely that it can take advantage of the ditopic nature of the receptors. Indeed, the crystal structure of the association of oxa^{2-} with $H_6btpN_7^{6+}$ (Figure 2) seems to support this assumption. Thus its higher association constant is probably due to the binding of both carboxylate groups to one of the head units of the receptors, in addition to its higher charge density that should also contribute to a stronger electrostatic interaction. In addition, the crystal structure of the oxa^{2-} association (Figure 2) suggests the possible presence of water molecules mediating the hydrogen-bonding network between the ammonium and carboxylate groups, compensating the smaller size of this dianion. The higher association constant of fum^{2-}, on the other hand, points to a better fit into the cavities in addition to its higher rigidity when compared to the other substrates. This is especially evident comparing fum^{2-} and suc^{2-} association behaviors. Although both carboxylates have about the same size being suc^{2-} more flexible, the binding of the latter is much weaker, the K_{eff} value at pH 4.5 is 1.65 log units lower in the case of its association with $H_nbtpN_7^{n+}$ and 1.79 log units lower in the case of $H_nt_2pN_8^{n+}$. In addition, $\pi-\pi$ interactions between the *p*-xylyl spacers of the receptors and the C=C bond of fum^{2-} may also contribute to the enhanced affinity.

Both receptors show the lowest affinity toward glu^{2-}, most likely because this is the longest and most flexible of the studied dicarboxylates. Interestingly, the K_{eff} value at pH 4.5 for the association of glu^{2-} with $H_nt_2pN_8^{n+}$ is still quite significant (3.16 log units).

The most interesting feature of the two receptors is their remarkable selectivity for fum^{2-} over its *cis* isomer $male^{2-}$ at pH ≈ 4, as shown in Figure 6. Indeed, few receptors were reported that effectively discriminate these *cis*/*trans* isomers; however, they all show selectivity for $male^{2-}$ over fum^{2-}.[11] In addition, the receptors described here are the only ones working in aqueous solution. The receptors rely on several features to achieve the observed discrimination. Structurally speaking, the ditopic nature and the length of the *p*-xylyl spacer of the receptors make them better suited for fum^{2-} as this substrate has an extended conformation due to the *trans* disposition of the carboxylate groups. The acid/base properties of the receptors also play a key role in the selectivity observed: both receptors are fully protonated at a pH value where fum^{2-} is completely deprotonated, thus bearing two negative charges, whereas maleate has only one negative charge at that pH.

It was expected that the increased rigidity imparted by the 2,4,6-triethylbenzene subunit of $H_nbtpN_7^{n+}$ would lead to a higher preorganization and consequently to stronger associations relative to $H_nt_2pN_8^{n+}$. Since the opposite occurred, it is reasonable to assume that the 2,4,6-triethylbenzene subunit does not sufficiently preorganize the receptor and consequently a rearrangement is necessary. This is evident in both crystal structures presented in Figures 2 and 3. In the crystal structure of the oxa^{2-} association, (Figure 2) one of the secondary ammonium groups of the 2,4,6-triethylbenzene subunit is turned outside of the cavity, and in the crystal structure of the fum^{2-} association (Figure 3) it is clear that two secondary ammonium groups of the tren subunit are turned outside of the cavity. These features clearly indicate that these crystal structures represent transient conformations which are between the encapsulated and the nonencapsulated states of the associations. The $H_nt_2pN_8^{n+}$ receptor should also require a conformational rearrangement upon binding (see Scheme 1); however, the energetic cost of such rearrangement should be higher in the case of $H_nbtpN_7^{n+}$, most likely due to the rigidity imparted by the 2,4,6-triethylbenzene subunit.

Additionally, it is known that removing polar solvent from charged sites requires significant amounts of enthalpic energy such that the stability of anion/receptor associations is mostly determined by favorable entropic terms produced by the desolvation of the interacting species.[17] In this regard, the binding of dicarboxylates by $H_nbtpN_7^{n+}$, which contains one more aromatic group than $H_nt_2pN_8^{n+}$, thus being more lipophilic, may be less favored by such desolvation processes than $H_nt_2pN_8^{n+}$.[18] Moreover, the electronic π cloud of the 2,4,6-triethylbenzene subunit may also repel the carboxylate group in some extent.

NMR Studies. The ^1H NMR spectra of solutions of equimolar amounts of the receptors and each dicarboxylate substrates in D_2O at pD = 4.50 were recorded (see Figures 7

dx.doi.org/10.1021/jo300320w | J. Org. Chem. 2012, 77, 4611−4621

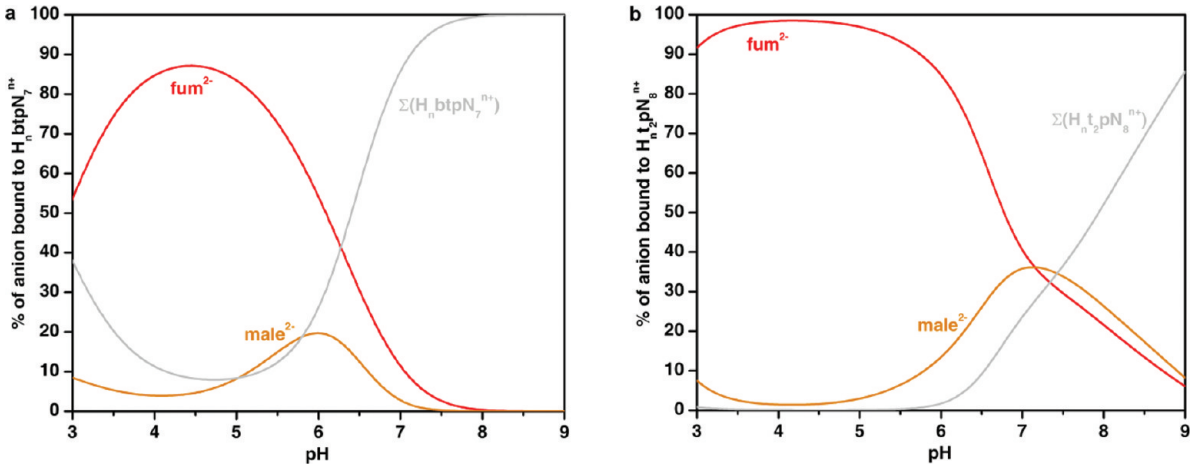

Figure 6. Distribution diagrams of the overall amounts of supramolecular species formed by fum^{2+} and male^{2+} anions with $H_nbtpN_7^{n+}$ (a) and $H_nt_2pN_8^{n+}$ (b) in equimolar ratio. $C_{btpN_7} = C_{t_2pN_8} = C_A/3 = 1.0 \times 10^{-3}$ M. For simplicity, the amount of associated species with each anion, $[H_nLA]^{(n-2)+}$, is identified in the diagrams only by the acronym of the anions, fum^{2-} and male^{2-}, respectively.

Scheme 1. Representation of Possible Conformational Rearrangement of $H_6btpN_7^{6+}$ and $H_6t_2pN_8^{6+}$ upon Dicarboxylate Binding

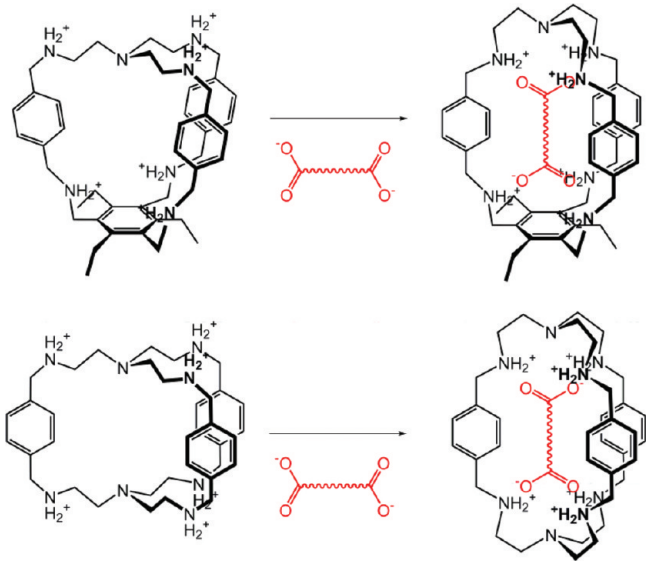

and 8). The number and integration of the signals observed in the spectra of $H_6btpN_7^{6+}$ and $H_6t_2pN_8^{6+}$ suggest highly symmetric structures in solution, consistent with averaged C_{3v} and C_{3h} symmetries, respectively. It should be noted however that the spectrum of $H_6btpN_7^{6+}$ exhibits broader peaks than that of $H_6t_2pN_8^{6+}$ suggesting that interconversion of different conformations are slower due to its higher rigidity.

In all cases, only one set of signals was observed for the free receptors and for the associated entities, indicating fast receptor−substrate exchanges on the NMR time scale. The signals of the protons of all substrates showed marked upfield shifts (whose magnitude correlate well with the calculated K_{eff} value at pH 4.5, see Figure 4), indicating that these atoms are inside the magnetically shielding region of the aromatic cavity (Figures 7 and 8, Table 3). As already observed in systems with receptors possessing cavities formed by aromatic walls, such large upfield shifts strongly suggest the encapsulation of the substrates.[19,20]

The chemical shifts of the receptors protons are not as affected by binding as those of the substrates, a consequence of the highly symmetric nature of the compounds. In addition, interpretation of the direction of the shift of these signals is not straightforward as it depends on several factors which may operate in opposite directions, namely hydrogen bond formation, desolvation effects and association induced conformational changes in the receptors. Nonetheless, it is clear that signals of protons close to the ammonium groups (e, f, i, and j in the case of $H_6btpN_7^{6+}$; e and f in $H_6t_2pN_8^{6+}$) exhibit larger shifts and their magnitude is proportional to the calculated K_{eff} value at pH 4.5 (Figure 4).

The spectra of the $H_6btpN_7^{6+}$ associations with the dicarboxylate anions carry more information than those of $H_6t_2pN_8^{6+}$ because it is possible to distinguish protons on the tren cap side from those of the 2,4,6-triethylbenzene head unit. With this in mind, it is possible to observe that the most shifted resonances by the association with fum^{2-} correspond to e, i, g, and h protons in agreement with the fact that this anion takes advantage of the ditopic nature of the receptor. In the oxa^{2-} association, peaks of e and j protons are also the most affected indicating that oxa^{2-} is interacting with both heads of the receptor. Because oxa^{2-} is much shorter than fum^{2-}, this one fitting well inside the receptor cavity, it is possible that oxa^{2-} moves fast inside the cavity interacting with one side of the receptor at a time or water molecules mediate hydrogen-bonding which can compensate the smaller size of this dianion, as seen on the crystal structure in Figure 2. A Job's plot confirmed 1:1 receptor:oxa^{2-} stoichiometry, ruling out the possibility of two encapsulated oxa^{2-} anions (Figure S2 in the Supporting Information). Both fum^{2-} and oxa^{2-} binding cause sharpening of the receptors proton resonances possibly by favoring a single conformation or a smaller set of conformations of the receptor.

■ CONCLUSION

Solution studies showed that $H_nbtpN_7^{n+}$ and $H_nt_2pN_8^{n+}$ receptors are able to strongly bind dicarboxylate substrates in highly competitive aqueous medium. Although $H_nt_2pN_8^{n+}$ has much higher affinity toward dicarboxylates than the structurally similar $H_nbtpN_7^{n+}$, their selectivity pattern is nearly identical. Therefore, the higher affinity did not give rise to enhanced

dx.doi.org/10.1021/jo300320w | J. Org. Chem. 2012, 77, 4611−4621

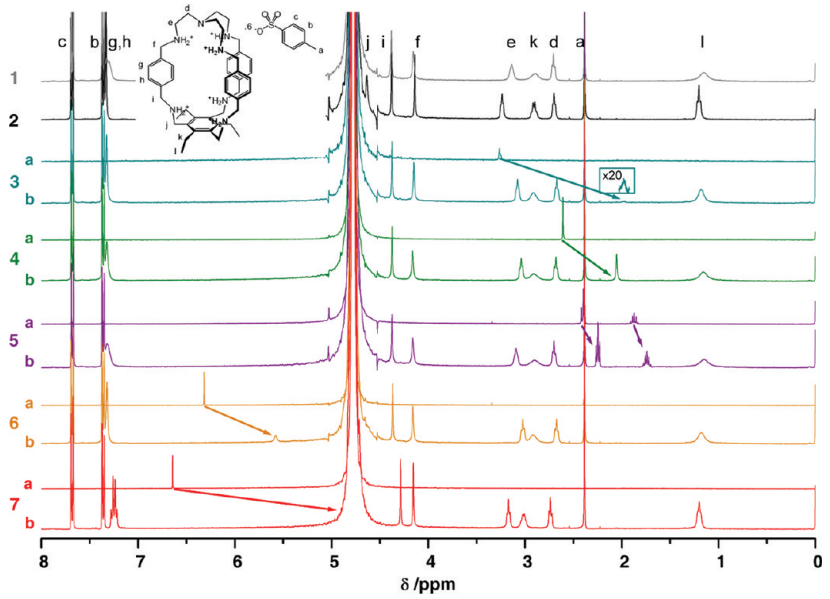

Figure 7. ^{1}H NMR spectra of solutions of the $H_6btpN_7(TsO)_6$ free receptor (**1**), free substrates, mal^{2-} (**3a**), suc^{2-} (**4a**), glu^{2-} (**5a**), $male^{2-}$ (**6a**), and fum^{2-} (**7a**) and of the association of the receptor with each dicarboxylate substrate in equimolar amounts, oxa^{2-} (**2**), mal^{2-} (**3b**), suc^{2-} (**4b**), glu^{2-} (**5b**), $male^{2-}$ (**6b**), and fum^{2-} (**7b**), in D_2O at pD = 4.5 and 298.2 K.

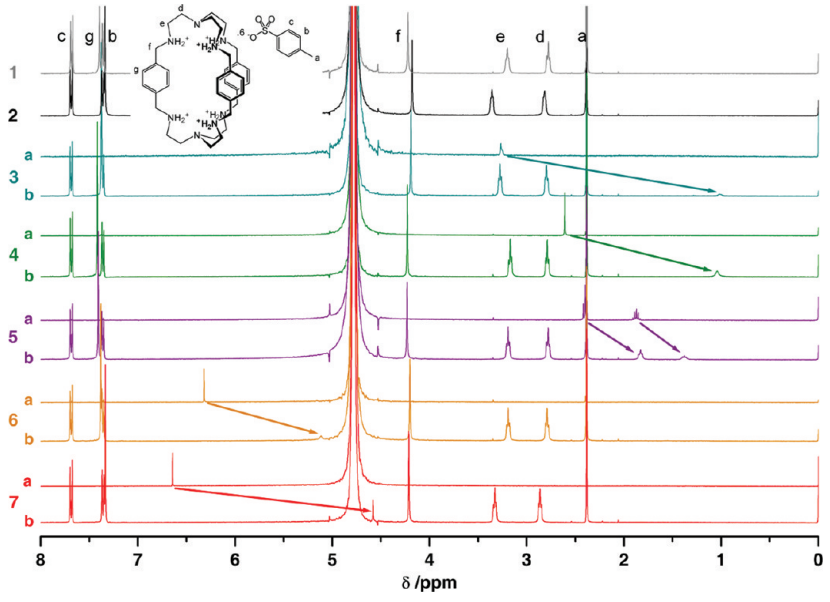

Figure 8. ^{1}H NMR spectra of solutions of the $H_6t_2pN_8(TsO)_6$ free receptor (**1**), free substrates, mal^{2-} (**3a**), suc^{2-} (**4a**), glu^{2-} (**5a**), $male^{2-}$ (**6a**), and fum^{2-} (**7a**) and of the association of the receptor with each dicarboxylate substrate in equimolar amounts, oxa^{2-} (**2**), mal^{2-} (**3b**), suc^{2-} (**4b**), glu^{2-} (**5b**), $male^{2-}$ (**6b**), and fum^{2-} (**7b**), in D_2O at pD = 4.5 and 298.2 K.

selectivity as might be expected. The identical selectivity pattern results from the fact that the two binding subunits in both compounds are separated by the same distance, defined by the *p*-xylyl spacer, yielding identical cavities in terms of size and number of binding units. Therefore, the enthalpy of binding of a given substrate, which arises mainly from electrostatic attraction and hydrogen bond formation, should be very similar in both receptors.

The large difference in affinity for the associations of dicarboxylates with $H_nbtpN_7^{n+}$ and with $H_nt_2pN_8^{n+}$ should be related with the energetic cost of conformational rearrangement upon binding. In this view, the 2,4,6-triethylbenzene cap of $H_nbtpN_7^{n+}$ is responsible for a more costly conformational rearrangement and thus lower affinity.

In both receptors, oxa^{2-} and fum^{2-} display the largest association constants than the rest of the substrates. This is related with differences in basicity of the substrates however structural features also play an important role. The fum^{2-} anion appears to have the right size, shape and rigidity to fit into the cavities of the receptors, while the oxa^{2-} large association constant is related with its higher charge density combined with possible water mediated hydrogen-bonding to compensate the smaller size of this dianion. The other studied anions, mal^{2-}, suc^{2-}, glu^{2-}, and $male^{2-}$, are bound less strongly, although the ^{1}H NMR studies showed marked upfield shifts in the proton

dx.doi.org/10.1021/jo300320w | *J. Org. Chem.* 2012, 77, 4611−4621

Table 3. Chemical Shifts ($\Delta\delta$)[a] and Respective Effective Association Constants (K_{eff})[b] for the Binding of Dicarboxylate Substrates by $H_n btpN_7^{n+}$ and $H_n t_2pN_8^{n+}$

	L = $btpN_7$		L = t_2pN_8	
	$\Delta\delta$ (ppm)	log K_{eff}	$\Delta\delta$ (ppm)	log K_{eff}
$H_nLoxa^{(n-2)+}$		3.89		6.03
$H_nLmal^{(n-2)+}$	1.28	2.83	2.25	4.42
$H_nLsuc^{(n-2)+}$	0.55	2.10	1.57	3.72
$H_nLglu^{(n-2)+}$	0.15	1.76	0.57	3.16
$H_nLmale^{(n-2)+}$	0.74	2.29	1.21	3.86
$H_nLfum^{(n-2)+}$	1.8 ± 0.3[c]	3.70	2.06	5.81

[a]Calculated upfield chemical shifts induced by binding on the α-CH_2 or vinylic protons of the substrate in D_2O and pD = 4.5. [b]Calculated for pH = 4.5 using the association constants determined in H_2O at T = (298.2 ± 0.1) K and I = (0.10 ± 0.01) M in KTsO. [c]In this case, the vinylic protons of associated fum^{2-} appear under the solvent peak, and therefore, it is not possible to determine a more precise value.

signals of all substrates with both receptors, indicating that they are inside the magnetically shielding region of the aromatic cavity, strongly suggesting encapsulation or at least close proximity to the entrance of the cavity. The lower affinity of mal^{2-}, suc^{2-}, glu^{2-}, and $male^{2-}$ may be ascribed to worse fit to the cavity arising from their own conformational preferences and flexibility, which may not allow them to take advantage of all the possible interactions that the receptors can provide. A less than perfect match will result in an amount of energetic gain which may not be enough to compensate the cost of conformational rearrangement of both binding partners contributing to lower association constants. The comparison between the association constants of fum^{2-} and suc^{2-}, both having the same number of carbon atoms, which are larger for fum^{2-} with both receptors, clearly shows that suc^{2-} requires additional conformational rearrangement due to its higher flexibility, resulting in a smaller association constant.

In addition, it was found that the two receptors show selectivity for fum^{2-} over its *cis* isomer $male^{2-}$ at pH ≈ 4.5. This is to the best of our knowledge the first synthetic receptors that can effectively discriminate these *cis*/*trans* isomers in aqueous solution, with a preference for fum^{2-}.

In conclusion, the present study shows that selectivity is not necessarily enhanced by high affinity, contrary to what might be expected, and that the increased rigidity can only result in increased affinity when no rearrangement is necessary upon binding, that is, when the receptor is preorganized.

EXPERIMENTAL SECTION

General Considerations. All solvents and chemicals were commercially purchased reagent grade quality and used as supplied without further purification. The compounds $btpN_7$ and t_2pN_8 were synthesized according to previously reported procedures.[13,21] The purity of both compounds was confirmed by ^1H NMR (Figures S3 and S4 in the Supporting Information) and elemental analysis. For the compound $btpN_7$: ^1H NMR (400 MHz, $CDCl_3$, 298 K; Me_4Si) δ = 6.81, 6.69, 3.94, 3.60, 3.37, 2.96, 2.53, 2.43, 1.69, 1.23, 1.12. Anal. Calcd for $C_{45}H_{63}N_7$: C, 77.0; H, 9.0; N, 14.0. Found: C, 76.7; H, 8.9; N, 13.9. For the compound t_2pN_8: ^1H NMR (400 MHz, $CDCl_3$, 298 K; Me_4Si) δ = 7.26, 3.68, 2.83, 2.66, 1.71. Anal. Calcd for $C_{36}H_{54}N_8$: C, 72.2; H, 9.1; N, 18.7. Found: C 72.3, H 8.7, N 18.7. Potassium *p*-toluenesulfonate (KTsO) was prepared by the neutralization of HTsO with KOH in water, followed by recrystallization from H_2O/MeOH. NMR spectra used for characterization of products and in the NMR studies were recorded on a 400 MHz instrument. TMS was used as reference for the ^1H NMR measurements in $CDCl_3$ and in D_2O the 3-(trimethylsilyl)propanoic acid-d_4–sodium salt. Peak assignments are based on peak integration and multiplicity for 1D ^1H spectra and on COSY, NOESY and HMQC experiments.

$[H_6btpN_7(H_2O)_2](oxa)_3\cdot 11H_2O$ and $[(H_5btpN_7^{5+}(H_2O)_4)_2(fum)_5]\cdot 36H_2O\cdot MeOH$ Crystals. The compound $btpN_7$ (3.5 mg, 5.0 μmol) was dissolved in a solution of 0.025 M H_2A (600 μL) (A = oxa or fum) after which the solution was concentrated to about 250 μL. Methanol was carefully added (500 μL) in order to form two phases. Single colorless crystals for X-ray crystallographic determination were obtained overnight.

Potentiometric Measurements. *Reagents and Solutions.* All the solutions were prepared using demineralised water (obtained by a Millipore/Milli-Q system). A stock solution of the receptor was prepared at ca. 2.0 × 10^{-3} M. Stock solutions of the dicarboxylic acids (analytical grade) were prepared at about 2.5 × 10^{-2} M, and the concentrations were checked by titration with standard 0.100 M KOH solutions. Carbonate-free solutions of the KOH titrant were prepared from a Merck ampule diluted to 1000 mL with water (freshly boiled for about 2 h and allowed to cool under nitrogen). These solutions were discarded every time carbonate concentration was about 0.5% of the total amount of base. The titrant solutions were standardized (tested by Gran's method).[22]

Equipment and Working Conditions. The equipment used was described previously.[10b] The ionic strength of the experimental solutions was kept at 0.10 ± 0.01 M with KTsO, and the temperature was maintained at 298.2 ± 0.1 K. Atmospheric CO_2 was excluded from the titration cell during experiments by passing purified nitrogen across the top of the experimental solution.

Measurements. The $[H^+]$ of the solutions was determined by the measurement of the electromotive force of the cell, $E = E^{\circ\prime} + Q \log [H^+] + E_j$. The term pH is defined as $-\log [H^+]$. $E^{\circ\prime}$, Q, E_j, and K_w were determined by titration of a solution of known hydrogen-ion concentration at the same ionic strength, using the acid pH range of the titration. The liquid-junction potential, E_j, was found to be negligible under the experimental conditions used. The value of K_w was determined from data obtained in the alkaline range of the titration, considering $E^{\circ\prime}$ and Q valid for the entire pH range and found to be equal to $10^{-13.76}$ under our experimental conditions. Before and after each set of titrations, the glass electrode was calibrated as a $[H^+]$ probe by titration of 1.0 × 10^{-3} M standard HCl solution with standard KOH. Potentiometric equilibrium measurements were carried out by titrating a solution consisting in 20.00 mL of ~2.0 × 10^{-3} M $btpN_7$ solution diluted to a final volume of 40.00 mL, with standard KOH. Measurements were done with 0.10 M KTsO and 0.10 M KBr. The exact amount of $btpN_7$ was obtained by determination of the excess of acid present in a mixture of $btpN_7$ and *p*-toluenesulfonic acid 1.4 × 10^{-2} M by titration with standard KOH solution. The protonation constants of t_2pN_8 were determined by titration of 20.00 mL of ~2.0 × 10^{-3} M compound solution (in the free base form) diluted to a final volume of 40.00 mL, with standard HTsO solution, because t_2pN_8 is insoluble below pH 4.8 in 0.10 M KTsO medium. For this reason a titration was performed in 0.05 M KTsO which allowed the determination of the exact amount of t_2pN_8 and to check that the protonation of both tertiary amines of t_2pN_8 could not take place in the 2.5–4.8 pH region. Potentiometric equilibrium measurements were then carried out with both compounds in the presence of each substrate at 1:3 R/S ratios (R = receptor and S = substrate). No solubility problems where found in the titrations of t_2pN_8 in the presence of the dicarboxylate substrates throughout the whole studied pH range in 0.10 M KTsO medium. In each titration about 100 points were collected, and a minimum of two titration curves were performed.

Calculation of Equilibrium Constants. Overall protonation constants, β_i^H, of ligands and anions, were calculated by fitting the potentiometric data obtained for all the performed titrations in the same experimental conditions with the HYPERQUAD program.[23] All these constants were taken as fixed values to obtain the equilibrium constants of the new species from the experimental data corresponding to all the titrations at 1:3 R/A ratio, also using the HYPERQUAD

dx.doi.org/10.1021/jo300320w | J. Org. Chem. 2012, 77, 4611–4621

program. The initial computations were obtained in the form of overall stability constants, $\beta_{H_hLlA_a}$ values, $\beta_{H_hLlA_a} = [H_hL_lA_a]/[H]^h[L]^l[A]^a$. The errors quoted are the standard deviations of the overall association constants given directly by the program for the input data, which include all the experimental points of all titration curves. The HYSS program[24] was used to calculate the concentration of equilibrium species from the calculated constants from which distribution diagrams were plotted. The species considered in a particular model were those that could be justified by the principles of supramolecular chemistry.

NMR studies. Solutions of $H_6btpN_7(TsO)_6$, $H_6t_2pN_8(TsO)_6$, free dicarboxylate substrates, and respective associations were prepared in D_2O in 2.0×10^{-3} M concentration, and the pD was adjusted to 4.5 by addition of DTsO or KOD with an Orion 420A instrument fitted with a combined Ingold 405M3 microelectrode. The pH*, the reading of the pH meter previously calibrated with two standard aqueous buffers at pH 4 and 8, was measured directly in the NMR tube. The final pD was calculated from pD = pH* + (0.40 ± 0.02).[25]

Job's Plot. Stock solutions of 2.0×10^{-3} M $(H_6btpN_7)(TsO)_6$ and K_2oxa were prepared in D_2O. Ten NMR tubes were prepared having a total concentration of $(H_6btpN_7)(TsO)_6$ and of K_2oxa maintained at 2.0×10^{-3} M. The pD value was adjusted to 4.50 with DTsO or KOD. The chemical shift changes for each solution were measured, and the product between the increment in chemical shift and receptor concentration versus the molar fraction of the receptor was plotted. A curve is generated where the maximum point indicates the stoichiometry of the association by use of the equation, $[C] = [R]_0(\delta_{obs} - \delta_R)/(\delta_{max} - \delta_R)$, where $[R]_0$ is the total receptor concentration, δ_{obs} is the observed chemical shift, δ_R is the chemical shift of the free receptor, and δ_{max} is the chemical shift of the cryptate. Because $\delta_{max} - \delta_R$ is a constant, the concentration of the associated entity is proportional to $\Delta\delta[R]_0$ (where $\Delta\delta = \delta_{obs} - \delta_R$). Plots of $\Delta\delta X_R$ as a function of X_R (where X_R is the molar fraction of the receptor) that exhibit a maximum at $X_R = 0.5$, indicating a 1:1 association.

Crystallography. The X-ray data of the anion associations were collected on at 150(2) K using graphite-monochromatized Mo Kα radiation (λ = 0.71073 Å). The crystal of $[H_6btpN_7(H_2O)_2](oxa)_3 \cdot 11H_2O$ was positioned at 35 mm from the CCD, the spots were measured using a counting time of 30 s, the crystal of $[(H_5btpN_7^{5+}\text{-}(H_2O)_4)_2(fum)_5] \cdot 36H_2O \cdot MeOH$ was positioned at 40 mm from the CCD, and the spots were measured using a counting time of 100 s. Data reduction including a multiscan absorption correction was carried out using the SAINT-NT software package. The structures were solved by a combination of direct methods with subsequent difference Fourier syntheses and refined by full matrix least-squares on F^2 using the SHELX-97 suite.[26] Anisotropic thermal displacements were used for all non-hydrogen atoms. The atomic positions of the water hydrogen atoms for oxa^{2-} association were obtained from the last Fourier maps apart of those of one water molecule. The hydrogen atoms of this molecule as well as those from crystallization water molecules of the fum^{2-} association were not taking into account in the structure refinement. The remaining hydrogen atoms were inserted at geometrical positions with exception of that from N–H secondary amine group in fum^{2-} association, which was also taken from a Fourier Map. Individual isotropic temperature factors were used for N–H hydrogen atoms and constrained isotropic temperature factors for C–H and O–H ones ($U_{iso} = 1.2U_{eq}$ to those they are attached). Molecular diagrams were drawn with PYMOL[27] and PLATON[28] software packages. The crystal data and refinement details are summarized in Table S6 given in the Supporting Information.

■ ASSOCIATED CONTENT

Supporting Information

^{1}H NMR of the studied compounds; table with stepwise protonation constants of $btpN_7$; table with overall and stepwise protonation constants of the studied dicarboxylate anions; table with the overall association constants (log $\beta_{H_hL_lA_a}$); Job's plot; tables of hydrogen bonding parameters of the crystal structures; table with the crystal data and selected refinement details. This material is available free of charge via the Internet http://pubs.acs.org.

■ AUTHOR INFORMATION

Corresponding Author

*Tel: (+351) 21 446 9737. Fax: (+351) 21 441 1277. E-mail: delgado@itqb.unl.pt.

Notes

The authors declare no competing financial interest.

■ ACKNOWLEDGMENTS

The NMR spectrometers are part of the National NMR Network and were purchased in the framework of the National Program for Scientific Re-equipment, Contract No. REDE/1517/RMN/2005, with funds from POCI 2010 (FEDER) and Fundação para a Ciência e a Tecnologia (FCT). We also acknowledge M. C. Almeida for providing elemental analysis and ESI-MS data from the Elemental Analysis and Mass Spectrometry Service at the ITQB/IBET. P.M. thanks FCT for the grant (SFRH/BD/36159/2007).

■ REFERENCES

(1) (a) Bianchi, A.; Bowman-James, K.; Garcia-España, E. *Supramolecular Chemistry of Anions*; Wiley-VCH: New York, 1997. (b) Gale, P. A.; Quesada, R. *Coord. Chem. Rev.* **2006**, *250*, 3219–3244. (c) Gale, P. A.; García-Garrido, S. E.; Garric, J. *Chem. Soc. Rev.* **2008**, *37*, 151–190. (d) Caltagirone, C.; Gale, P. A. *Chem. Soc. Rev.* **2009**, *38*, 520–563. (e) Gale, P. A. *Chem. Soc. Rev.* **2010**, *39*, 3746–3771.

(2) Berg, J. M.; Tymoczko, J. L.; Stryer, L. *Biochemistry*, 5th ed.; W. H. Freeman: New York, 2002; pp 465–484.

(3) Brière, J.-J.; Favier, J.; Gimenez-Roqueplo, A.-P.; Rustin, P. *Am. J. Physiol. Cell Physiol.* **2006**, *291*, C1114–C1120.

(4) Ratcliffe, P. J. *Cancer Cell.* **2007**, *11*, 303–305.

(5) (a) Peczuh, M. W.; Hamilton, A. D. *Chem. Rev.* **2000**, *100*, 2479–2494. (b) Zhong, Z.; Anslyn, E. V. *Angew. Chem., Int. Ed.* **2003**, *42*, 3005–3008. (c) Gersthagen, T.; Schmuck, C.; Schrader, T. *Supramol. Chem.* **2010**, *22*, 853–861.

(6) (a) Kubik, S. *Chem. Soc. Rev.* **2010**, *39*, 3648–3663. (b) Rehm, T. H.; Schmuck, C. *Chem. Soc. Rev.* **2010**, *39*, 3597–3611.

(7) Fitzmaurice, R. J.; Kyne, G. M.; Douheret, D.; Kilburn, J. D. *J. Chem. Soc., Perkin Trans. 1* **2002**, 841–864.

(8) (a) Bianchi, A.; Micheloni, M.; Paoletti, P. *Coord. Chem. Rev.* **1991**, *110*, 17–113. (b) Dietrich, B. *Pure Appl. Chem.* **1993**, *65*, 1457–1464. (c) Ilioudis, C. A.; Steed, J. W. *J. Supramol. Chem.* **2001**, *1*, 165–187. (d) Llinares, J. M.; Powell, D.; Bowman-James, K. *Coord. Chem. Rev.* **2003**, *240*, 57–75. (e) McKee, V.; Nelson, J.; Town, R. M. *Chem. Soc. Rev.* **2003**, *32*, 309–325. (f) Bowman-James, K. *Acc. Chem. Res.* **2005**, *38*, 671–678. (g) Kubik, S.; Reyheller, C.; Stüwe, S. *J. Inclusion Phenom. Macrocycl. Chem.* **2005**, *52*, 137–187. (h) García-España, E.; Díaz, P.; Llinares, J. M.; Bianchi, A. *Coord. Chem. Rev.* **2006**, *250*, 2952–2988. (i) Wichmann, K.; Antonioli, B.; Söhnel, T.; Wenzel, M.; Gloe, K.; Price, J. R.; Lindoy, L. F.; Blake, A. J.; Schröder, M. *Coord. Chem. Rev.* **2006**, *250*, 2987–3003. (j) Katayev, E. A.; Ustynyuk, Y. A.; Sessler, J. L. *Coord. Chem. Rev.* **2006**, *250*, 3004–3037. (k) Bazzicalupi, C.; Bencini, A.; Lippolis, V. *Chem. Soc. Rev.* **2010**, *39*, 3709–3728.

(9) (a) Kang, S. O.; Llinares, J. M.; Day, V. W.; Bowman-James, K. *Chem. Soc. Rev.* **2010**, *39*, 3980–4003. (b) Mateus, P.; Bernier, N.; Delgado, R. *Coord. Chem. Rev.* **2010**, *254*, 1726–1747. (c) Ballester, P. *Chem. Soc. Rev.* **2010**, *39*, 3810–3830.

(10) (a) Arunachalam, M.; Ravikumar, I.; Ghosh, P. *J. Org. Chem.* **2008**, *73*, 9144–9147. (b) Mateus, P.; Delgado, R.; Brandão, P.; Carvalho, S.; Félix, V. *Org. Biomol. Chem.* **2009**, *7*, 4661–4673. (c) Mateus, P.; Delgado, R.; Brandão, P.; Félix, V. *J. Org. Chem.* **2009**, *74*, 8638–8646.

(11) (a) Sancenón, F.; Martínez-Máñez, R.; Miranda, M. A.; Seguí, M.-J.; Soto, J. *Angew. Chem., Int. Ed.* **2003**, *42*, 647–650. (b) Yen,

Y.-P.; Ho, K.-W. *Tetrahedron Lett.* **2006**, *47*, 7357−7361. (c) Costero, A. M.; Colera, M.; Gavin, P.; Gil, S. *Chem. Commun.* **2006**, 761−763. (d) Tseng, Y.-P.; Tu, G.-M.; Lin, C.-H.; Chang, C.-T.; Lin, C.-Y.; Yen, Y.-P. *Org. Biomol. Chem.* **2007**, *5*, 3592−3598. (e) Lin, Y.-S.; Tu, G.-M.; Lin, C.-Y.; Chang, Y.-T.; Yen, Y.-P. *New J. Chem.* **2009**, *33*, 860−867.

(12) (a) Motekaitis, R. J.; Martell, A. E.; Lehn, J.-M.; Watanabe, E.-I. *Inorg. Chem.* **1982**, *21*, 4253−4251. (b) Aguilar, J.; Clifford, T.; Danby, A.; Llinares, J. M.; Mason, S.; García-España, E.; Bowman-James, K. *Supramol. Chem.* **2001**, *13*, 405−417. (c) Dietrich, B.; Guilhem, J.; Lehn, J.-M.; Pascard, C.; Sonveau, E. *Helv. Chim. Acta* **1984**, *67*, 91−104. (d) Heyer, D.; Lehn, J.-M. *Tettrahedron Lett.* **1986**, *27*, 5869−5672. (e) Hynes, M. J.; Maubert, B.; McKee, V.; Town, R. M.; Nelson, J. *J. Chem. Soc., Dalton Trans.* **2000**, 2853−2859. (f) Clifford, T.; Danby, A.; Llinares, J. M.; Mason, S.; Alcock, N. W.; Powell, D.; Aguilar, J. A.; García-España, E.; Bowman-James, K. *Inorg. Chem.* **2001**, *40*, 4710−4720.

(13) Mateus, P.; Delgado, R.; Brandão, P.; Félix, V. *Chem.—Eur. J.* **2011**, *17*, 7020−7031.

(14) Li, Y.; Jiang, L.; Feng, X.-L.; Lu, T.-B. *Cryst. Growth Des.* **2008**, *8*, 3689−3694.

(15) Albelda, M. T.; Bernardo, M. A.; García-España, E.; Godino-Salido, M. L.; Luis, S. V.; Melo, M. J.; Pina, F.; Soriano, C. *J. Chem. Soc., Perkin Trans. 2* **1999**, 2545−2549.

(16) Bianchi, A.; García-España, E. *J. Chem. Educ.* **1999**, *76*, 1727−1732.

(17) Schmidtchen, F. P. *Coord. Chem. Rev.* **2006**, *250*, 2918−2928.

(18) Arranz, P.; Bencini, A.; Bianchi, A.; Diaz, P.; García-España, E.; Giorgi, C.; Luis, S. V.; Querol, M.; Valtancoli, B. *J. Chem. Soc., Perkin Trans. 2* **2001**, 1765−1770.

(19) Kintzinger, J.-P.; Kotzyba-Hibert, F.; Lehn, J.-M.; Pagelot, A.; Saigo, K. *J. Chem. Soc., Chem. Commun.* **1981**, 833−836.

(20) Lehn, J.-M.; Meric, R.; Vigneron, J.-P.; Waksman, I. B.; Pascard, C. *J. Chem. Soc., Chem. Commun.* **1991**, 62−64.

(21) Lakshminarayanan, P. S.; Ravikumar, I.; Suresh, E.; Ghosh, P. *Cryst. Growth Des.* **2008**, *8*, 2842−2852.

(22) Rossotti, F. J.; Rossotti, H. J. *J. Chem. Educ.* **1965**, *42*, 375−378.

(23) Gans, P.; Sabatini, A.; Vacca, A. *Talanta* **1996**, *43*, 1739−1753.

(24) Alderighi, L.; Gans, P.; Ienco, A.; Peters, D.; Sabatini, A.; Vacca, A. *Coord. Chem. Rev.* **1999**, *184*, 311−318.

(25) Delgado, R.; da Silva, J. J. R. F.; Amorim, M. T. S.; Cabral, M. F.; Chaves, S.; Costa, J. *Anal. Chim. Acta* **1991**, *245*, 271−282.

(26) Sheldrick, G. M. *Acta Crystallogr.* **2008**, *A64*, 112−122.

(27) The PyMOL Molecular Graphics System, Version 1.2r3pre, Schrödinger, LLC.

(28) Spek, A. L. *J. Appl. Crystallogr.* **2003**, *36*, 7−13.